On particle–particle interactions in solid, non-conducting impurity removal

Antoine Sellier

LadHyX, École polytechnique, 91128 Palaiseau cedex, France

Abstract

A whole boundary-integral formulation is proposed to determine the rigid-body motions of two solid and insulating particles, freely-suspended in a metal liquid and subject to uniform ambient electric and magnetic fields. As revealed by our numerical results, particle–particle interactions may become significant for close enough bodies. *To cite this article: A. Sellier, C. R. Mecanique 331 (2003).*
© 2003 Académie des sciences. Published by Éditions scientifiques et médicales Elsevier SAS. All rights reserved.

Résumé

Sur l'interaction particule–particule lors de l'extraction d'impuretés solides isolantes. En s'appuyant sur une formulation intégrale, on détermine le mouvement de deux particules solides, isolantes et plongées dans un métal liquide, sous l'action conjuguée d'un champ électrique et d'un champ magnétique uniformes. Les premiers résultats numériques montrent que les interactions entre les particules peuvent être très fortes lorsque ces dernières s'avèrent proches. *Pour citer cet article : A. Sellier, C. R. Mecanique 331 (2003).*
© 2003 Académie des sciences. Published by Éditions scientifiques et médicales Elsevier SAS. All rights reserved.

1. Introduction

As theoretically predicted [1] and further experimentally confirmed [2], a solid and insulating particle freely immersed in a Newtonian liquid metal of uniform density ρ, kinematic viscosity μ and conductivity $\sigma_l > 0$ moves under externally applied, steady and uniform electric and magnetic fields $\mathbf{E}$ and $\mathbf{B}$. As established in [1], a single sphere of radius a then does not rotate and translates at the following velocity

$$U = -\frac{\sigma_l a^2}{6\mu}\mathbf{E} \wedge \mathbf{B} \tag{1}$$

A general framework [3] and a theoretical procedure have been proposed and implemented for a single, non-conducting and arbitrarily-shaped particle in [4,5]. However, particle–particle interactions may become significant for close bodies. This study thus extends the prior works [4,5] to the case of two (close) insulating particles. The conditions of zero net force and torque on each particle are first expressed by using the reciprocal identity. The required velocity components are thus governed by a linear system which solely appeals on each particle boundary to the surface tractions induced by six specific Stokes flows and the first-order and second-order Cartesian derivatives of the perturbation potential. All these quantities are finally obtained by solving boundary-integral equations; a procedure which circomvents the calculation of the electric field and the flow in the unbounded fluid domain.

2. The governing integral formulation

As sketched in Fig. 1, let us consider two solid particles $\mathcal{P}_n$ ($n = 1, 2$), of insulating boundaries S_n, closely immersed in the conducting liquid metal occupying the unbounded domain Ω. We further denote by $\mathbf{n}$ the unit outward normal on the whole surface $S = S_1 \cup S_2$ and resort to Cartesian coordinates (O, x_1, x_2, x_3) and the usual tensor summation convention with $\mathbf{OM} = x_i \mathbf{e}_i$ and $r = (x_i x_i)^{1/2}$.

The particles modify the electric field which becomes $\mathbf{E} - \nabla\phi$ in the domain Ω. For our insulating surface S the potential ϕ obeys the well-posed exterior Neumann problem

$$\nabla^2\phi = 0 \quad \text{in } \Omega, \qquad \nabla\phi \to 0 \quad \text{as } r \to \infty, \qquad \nabla\phi \cdot \mathbf{n} = \mathbf{E} \cdot \mathbf{n} \quad \text{on } S_1 \cup S_2 \tag{2}$$

The unknown rigid-body motion of $\mathcal{P}_n$ is entirely described by its angular velocity $\boldsymbol{\Omega}^{(n)} = \Omega_j^{(n)} \mathbf{e}_j$ and the (translational) velocity $\mathbf{U}^{(n)} = U_j^{(n)} \mathbf{e}_j$ of its point O_n. Denoting by μ_0, V and a the uniform fluid electromagnetic permeability and the typical particles length and velocity scales, we assume that the associated Reynolds number Re, magnetic Reynolds number Re$_m$ and Hartmann number are small, i.e. that

$$\text{Re} = \rho V a / \mu \ll 1, \qquad \text{Re}_m = \mu_0 \sigma_l V a \ll 1, \qquad M = |\mathbf{B}| a (\sigma_l / \mu)^{1/2} \ll 1 \tag{3}$$

Thus [3], the magnetic field $\mathbf{B}$ is not disturbed and the Lorentz body force $\mathbf{f}$ in the fluid is $\mathbf{f} = \mathbf{A} - \sigma_l \nabla\phi \wedge \mathbf{B}$ where $\mathbf{A} = \sigma_l \mathbf{E} \wedge \mathbf{B}$ is uniform. In addition, the quasi-steady fluid flow of velocity $\mathbf{u}$ and pressure $p + \mathbf{A} \cdot \mathbf{OM}$ is such that

$$\nabla \cdot \mathbf{u} = 0, \qquad \mu \nabla^2 \mathbf{u} = \nabla p + \sigma_l \nabla\phi \wedge \mathbf{B} \quad \text{in } \Omega \tag{4}$$

$$(\mathbf{u}, p) \to (\mathbf{0}, 0) \quad \text{as } r \to \infty, \qquad \mathbf{u} = \mathbf{U}^{(n)} + \boldsymbol{\Omega}^{(n)} \wedge \mathbf{O_n M} \quad \text{on } S_n \tag{5}$$

If $\sigma(\mathbf{u}, p)$ is the stress tensor associated to $(\mathbf{u}, p)$ and $\mathcal{V}_n$ the volume of $\mathcal{P}_n$, the requirement of zero net hydrodynamic force and torque on each freely-suspended particle can then be written

$$\int_{S_n} \sigma(\mathbf{u}, p) \cdot \mathbf{n} \, dS_n = \mathcal{V}_n \mathbf{A}, \qquad \int_{S_n} \mathbf{O_n M} \wedge [\sigma(\mathbf{u}, p) \cdot \mathbf{n}] \, dS_n = -\mathbf{A} \wedge \int_{\mathcal{P}_n} \mathbf{O_n M} \, dv; \quad n = 1, 2 \tag{6}$$
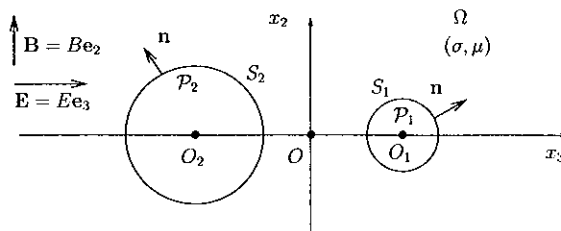

Fig. 1. Two solid and insulating inequal spheres in Case 1, i.e., when $(\mathbf{E}, \mathbf{B}) = (E\mathbf{e}_3, B\mathbf{e}_2)$.

Fig. 1. Deux sphères isolantes de tailles différentes dans le Cas 1, c'est-à-dire pour $(\mathbf{E}, \mathbf{B}) = (E\mathbf{e}_3, B\mathbf{e}_2)$.

As achieved in [4] for one particle, let us now introduce, for $L \in \{T, R\}$ and $n \in \{1, 2\}$, 12 steady Stokes flows $(\mathbf{u}_L^{(n),i}, p_L^{(n),i})$ free from body forces, quiescent far from O and such that

$$\mathbf{u}_T^{(n),i} = \delta_{nm}\mathbf{e}_i, \qquad \mathbf{u}_R^{(n),i} = \delta_{nm}[\mathbf{e}_i \wedge \mathbf{O_nM}] \quad \text{on } S_m \tag{7}$$

with $\delta_{nn} = 1$ and $\delta_{nm} = 0$ if $m \neq n$. Clearly, subscripts T or R are used for a translation or a rotation respectively of only one particle and the previous flows induce on S a surface force $\mathbf{f}_L^{(n),i} = \sigma(\mathbf{u}_L^{(n),i}, p_L^{(n),i}) \cdot \mathbf{n}$. Extending the usual reciprocal identity [6] to the multiply-connected surface S in presence of the decaying body force $-\sigma_l \nabla \phi \wedge \mathbf{B}$, one also obtains

$$\int_S [\mathbf{u}_L^{(n),i} \cdot \sigma(\mathbf{u}, p) \cdot \mathbf{n} - \mathbf{u} \cdot \mathbf{f}_L^{(n),i}] \, dS = F_L^{(n),i}, \qquad F_L^{(n),i} = -\sigma_l \int_\Omega \mathbf{u}_L^{(n),i} \cdot [\nabla \phi \wedge \mathbf{B}] \, d\Omega \tag{8}$$

Exploiting (8), the equalities (6) then yield the basic governing linear system

$$A_{(m),T}^{(n),i,j} U_j^{(m)} + B_{(m),T}^{(n),i,j} \Omega_j^{(m)} = \frac{1}{\mu} \left\{ -\sigma_l \mathcal{V}_{\mathcal{P}_n}[\mathbf{E} \wedge \mathbf{B}] \cdot \mathbf{e}_i + F_T^{(n),i} \right\} \tag{9}$$

$$A_{(m),R}^{(n),i,j} U_j^{(m)} + B_{(m),R}^{(n),i,j} \Omega_j^{(m)} = \frac{1}{\mu} \left\{ \sigma_l \left([\mathbf{E} \wedge \mathbf{B}] \wedge \left[\int_{\mathcal{P}_n} \mathbf{O_nM} \, dv \right] \right) \cdot \mathbf{e}_i + F_R^{(n),i} \right\} \tag{10}$$

if we adopt the following definitions

$$-\mu A_{(m),L}^{(n),i,j} = \int_{S_m} \mathbf{e}_j \cdot \mathbf{f}_L^{(n),i} \, dS_m, \qquad -\mu B_{(m),L}^{(n),i,j} = \int_{S_m} (\mathbf{e}_j \wedge \mathbf{O_mM}) \cdot \mathbf{f}_L^{(n),i} \, dS_m \tag{11}$$

Finally, it is possible to obtain a whole boundary formulation by converting each volume integral $F_L^{(n),i}$ into a surface integral. In the same spirit as in [4], one first notices that $\mathbf{u}_L^{(n),i}$ fortunately admits in the whole domain $\Omega \cup S$ the fruitful integral representation

$$[\mathbf{u}_L^{(n),i} \cdot \mathbf{e}_k](M) = -\int_S \left\{ \frac{\delta_{jk}}{PM} + \frac{(\mathbf{PM} \cdot \mathbf{e}_j)(\mathbf{PM} \cdot \mathbf{e}_k)}{PM^3} \right\} \left[\frac{\mathbf{f}_L^{(n),i} \cdot \mathbf{e}_j}{8\pi\mu} \right](P) \, dS; \quad k = 1, \dots, 3 \tag{12}$$

Injecting (12) in (8) and proceeding as in [4] (for conciseness, details are omitted here), one thus obtains the key decomposition

$$\frac{8\pi\mu}{\sigma_l} F_L^{(n),i} = -\int_S \int_S \mathbf{f}_L^{(n),i}(P) \cdot [\nabla\phi(M) \wedge \mathbf{B}] \frac{\mathbf{PM} \cdot \mathbf{n}(M)}{PM} \, dS_P \, dS_M$$

$$+ \int_S \int_S \left[\mathbf{f}_L^{(n),i}(P) \cdot \frac{\mathbf{PM}}{PM} \right] [\nabla\phi(M) \wedge \mathbf{B}] \cdot \mathbf{n}(M) \, dS_P \, dS_M$$

$$+ \int_S \int_S \varepsilon_{kmn} PM [\mathbf{f}_L^{(n),i} \cdot \mathbf{e}_k](P)[\mathbf{B} \cdot \mathbf{e}_n][\nabla(\phi_{,m}) \cdot \mathbf{n}](M) \, dS_P \, dS_M \tag{13}$$

where ε_{kmn} denotes the Cartesian component of the usual antisymmetric permutation tensor and the notation $\phi_{,m} = \partial\phi/\partial x_m$ is adopted. In summary, by virtue of (11) and (13) one only needs to compute the surface forces $\mathbf{f}_L^{(n),i}$, the gradient $\nabla\phi = \phi_{,m}\mathbf{e}_m$ and the normal fluxes $\nabla(\phi_{,m}) \cdot \mathbf{n}$ on the surface $S_1 \cup S_2$ when solving the linear system (9) and (10) of unknown generalized velocity $\mathbf{X} = (\mathbf{U}^{(1)}, \boldsymbol{\Omega}^{(1)}, \mathbf{U}^{(2)}, \boldsymbol{\Omega}^{(2)})$. It is thus no use to determine the fluid flow $(\mathbf{u}, p)$ and the potential ϕ in the unbounded domain Ω and we only appeal to surface quantities: this is the announced integral formulation of the problem. Note also that the system (9), (10) is well-posed: this admits a unique solution $\mathbf{X}$ because its 12×12 matrix is symmetric and positive-definite [7].

3. Advocated boundary-integral equations and numerical implementation

It is actually possible to compute all the required surface quantities $f_L^{(n),i}$, $\nabla\phi$ and $\nabla(\phi_{,m}) \cdot \mathbf{n}$ by resorting to a few boundary-integral equations on S as follows:

(1) by ensuring (12) on whole surface S in conjunction with (7) one readily obtains a Fredholm boundary-integral equation of the first kind on S for $f_L^{(n),i}$;

(2) recalling that any function ψ harmonic in Ω and decaying far from O at least as fast as $1/r$ fulfills (use the usual second Green's identity) the key boundary link

$$B_M[\psi] = D_M[\psi] - 4\pi\psi(M) = C_M[\nabla\psi \cdot \mathbf{n}] \quad \text{on } S \tag{14}$$

under the following definitions

$$D_M[v] = \int\limits_S \left[v(P) - v(M)\right]\frac{\mathbf{PM} \cdot \mathbf{n}(P)}{PM^3}\,\mathrm{d}S, \qquad C_M[v] = \int\limits_S \frac{v(P)}{PM}\,\mathrm{d}S \tag{15}$$

one also evaluates $\nabla\phi = \phi_{,m}\mathbf{e}_m$ and $\nabla(\phi_{,m}) \cdot \mathbf{n}$ on S by appealing to two steps:

(i) by virtue of (2), first select $\psi = \phi$ and determine ϕ on S by solving the Fredholm boundary-integral equation of the second kind $B_M[\phi] = d(M)$ with $d(M) = C_M[\nabla\phi \cdot \mathbf{n}]$ prescribed. The computation of tangential derivatives of ϕ on S thus gives the needed vector $\nabla\phi - (\nabla\phi \cdot \mathbf{n})\mathbf{n}$, i.e. (use (2)) the required gradient $\nabla\phi$ on the surface S;

(ii) finally, select $\psi = \phi_{,m}$ and thus deduce the normal flux $\nabla(\phi_{,m}) \cdot \mathbf{n}$ on S from the previous calculation of $\phi_{,m}$ on the surface by solving the Fredholm boundary-integral equation of the first kind $C_M[\nabla(\phi_{,m}) \cdot \mathbf{n}] = d_m(M)$ with $d_m(M) = B_M[\phi_{,m}]$ given by the previous step (i).

The numerical implementation resorts to a N_n-node mesh of 6-node triangular and curvilinear boundary elements on each surface S_n [6,8]. Each discretized counter-part of the previously mentioned boundary-integral equations results in a linear system of $N' \times N'$, dense and non-symmetric matrix (with $N' = N_1 + N_2$ or $N' = 3(N_1 + N_2)$), which is solved by a standard LU factorization algorithm. Each tangential derivative of ϕ on S is accurately evaluated by applying a refined fourth-order finite difference scheme to the computed values of ϕ.

4. Numerical results for 2-sphere clusters

This section presents our very first numerical results for 2-sphere clusters. More precisely, $\mathcal{P}_n$ is a sphere of radius a_n and center O_n with (see Fig. 1) $O_2O_1 = O_1O_2\mathbf{e}_3$, $a_2 \geqslant a_1$ and we take as length scale $a = a_1$. For a 2-sphere cluster only $\Omega_3^{(1)}$ and $\Omega_3^{(2)}$ are found to be non-zero if both $\mathbf{E}$ and $\mathbf{B}$ are aligned with the same vector $\mathbf{e}_i$. By superposition, we thus confine our attention to three cases

$$\text{Case 1: } (\mathbf{E}', \mathbf{B}') = (\mathbf{e}_3, \mathbf{e}_2), \quad \text{Case 2: } (\mathbf{E}', \mathbf{B}') = (\mathbf{e}_2, \mathbf{e}_3), \quad \text{Case 3: } (\mathbf{E}', \mathbf{B}') = (\mathbf{e}_1, \mathbf{e}_2) \tag{16}$$

with $|\mathbf{E}||\mathbf{B}| \neq 0$, $\mathbf{E}' = \mathbf{E}/|\mathbf{E}|$ and $\mathbf{B}' = \mathbf{B}/|\mathbf{B}|$. For those settings we look at the non-zero mobilities $u_j^{(n)}(\lambda)$ and $w_j^{(n)}(\lambda)$ such that

$$u_j^{(n)}(\lambda) = \frac{\mu U_j^{(n)}}{\sigma_s a^2 EB}, \qquad w_j^{(n)}(\lambda) = \frac{\mu\Omega_j^{(n)}}{\sigma_s a EB}, \qquad 0 \leqslant \lambda = \frac{a_1 + a_2}{O_1O_2} < 1 \tag{17}$$

where λ denotes the separation parameter.

As illustrated in Table 1 for $a_2 = 2a_1 = 2a$ and $\lambda = 0.1$ or $\lambda = 0.9$ in Case 2, the use of $N = N_1 = N_2$ collocation points on S_n for $a_2 \leqslant 2a_1$ ensures a 3-digit and a 4-digit accuracy for $u_j^{(n)}$ and $w_j^{(n)}$ respectively if $N = 530$ for $\lambda \geqslant 0.4$ and $N = 1058$ otherwise. Using these values of N, two clusters of equal ($a_2 = a_1$) and different ($a_2 = 2a_1$)

Table 1

Computed non-zero mobilities $u_1^{(n)}$ and $w_2^{(n)}$ in Case 2 for different numbers $N = N_1 = N_2$ of collocation points, $\lambda = 0.1$, $\lambda = 0.9$ and inequal spheres $(a_2 = 2a_1 = 2a)$

Tableau 1

Influence du nombre $N = N_1 = N_2$ de points de collocation pour les mobilités non nulles $u_1^{(n)}$ et $w_2^{(n)}$ dans le Cas 2 pour $\lambda = 0.1$, $\lambda = 0.9$ et deux sphères différentes $(a_2 = 2a_1 = 2a)$

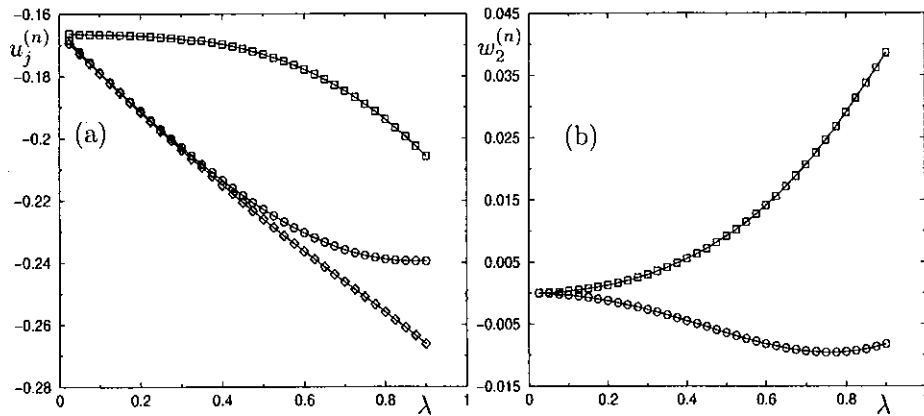| (N, λ)	$(242, 0.1)$	$(530, 0.1)$	$(1058, 0.1)$	$(242, 0.9)$	$(530, 0.9)$	$(1058, 0.9)$
$u_1^{(1)}$	-0.15703	-0.16323	-0.16620	-0.36356	-0.36519	-0.36560
$w_2^{(1)}$	0.00128	0.00118	0.00112	0.13596	0.13574	0.13574
$u_1^{(2)}$	-0.66146	-0.66471	-0.66643	-0.69862	-0.69927	-0.69962
$w_2^{(2)}$	-0.00022	-0.00017	-0.00014	-0.01652	-0.01634	-0.01633

Fig. 2. Non-zero mobilities for two equal spheres: (a) functions $-u_1^{(1)} = -u_1^{(2)}$ in Case 1 (O), $u_1^{(1)} = u_1^{(2)}$ in Case 2 (□) and $u_3^{(1)} = u_3^{(2)}$ in Case 3 (◇); (b) functions $w_2^{(1)} = -w_2^{(2)}$ in Case 1 (O) and Case 2 (□).

Fig. 2. Mobilités non nulles pour deux sphères identiques : (a) fonctions $-u_1^{(1)} = -u_1^{(2)}$ dans le Cas 1 (O), $u_1^{(1)} = u_1^{(2)}$ dans le Cas 2 (□) et $u_3^{(1)} = u_3^{(2)}$ dans le Cas 3 (◇) ; (b) fonctions $w_2^{(1)} = -w_2^{(2)}$ dans les Cas 1 (O) et 2 (□).

spheres are addressed. For symmetry reasons, in each above Cases 1–3 identical spheres $(a_2 = a_1)$ adopt opposite angular velocities $(\mathbf{\Omega}^{(1)} + \mathbf{\Omega}^{(2)} = \mathbf{0})$ and equal translational velocities $(\mathbf{U}^{(1)} = \mathbf{U}^{(2)})$, i.e., move with a constant center-to-center spacing $d = O_1 O_2 > 2a_1$. The associated non-zero mobilities $u_j^{(n)}(\lambda)$ and $w_j^{(n)}(\lambda)$ are displayed in Fig. 2 versus the separation parameter $\lambda = 2a_1/d$.

Of course, as $\lambda \to 0$ (d large) one recovers the solution (1) for a single sphere of radius $a = a_1$. For any Cases 1–3 the 2-sphere cluster translates parallel to $\mathbf{E} \wedge \mathbf{B}$ and faster than a single sphere. As shown in Fig. 2(a), the non-zero mobilities $u_j^{(n)}$ increase in magnitude as sphere approach (as $\lambda \to 1$) and for a given separation parameter λ admit the largest and smallest values for Cases 3 and 2 respectively. The spheres are free from rotation in Case 3 and rotate parallel to $\mathbf{e}_2$ at opposite angular velocities in other cases. As revealed by Fig. 2(b), $w_2^{(1)}$ increases from zero with λ in Case 2 and remains negative and of weak magnitude whatever λ in Case 1.

The cluster consisting of different spheres $(a_2 = 2a_1)$ exhibits a less simple behavior: this time the translational velocities $\mathbf{U}^{(1)}$ and $\mathbf{U}^{(2)}$ differ and the center-to-center distance $d = O_1 O_2$ will then change as the cluster moves. More precisely (see Fig. 3), the solution (1) still holds for $\lambda = 0$ and, as depicted in Fig. 3(a), each sphere again translates in any Case 1–3 parallel to $\mathbf{E} \wedge \mathbf{B}$, faster than when isolated and faster or slower than in Case 1 in Cases 3 and 2 respectively. However, the small sphere mobility $u_j^{(1)}(\lambda)$ may strongly differ from the mobility $u_j^{(1)}(0)$ of the single sphere as λ increases: in Cases 1 and 3 one obtains $|u_j^{(1)}(\lambda)/u_j^{(1)}(0)| \sim 4$ as $\lambda \to 0.9$. By contrast, the

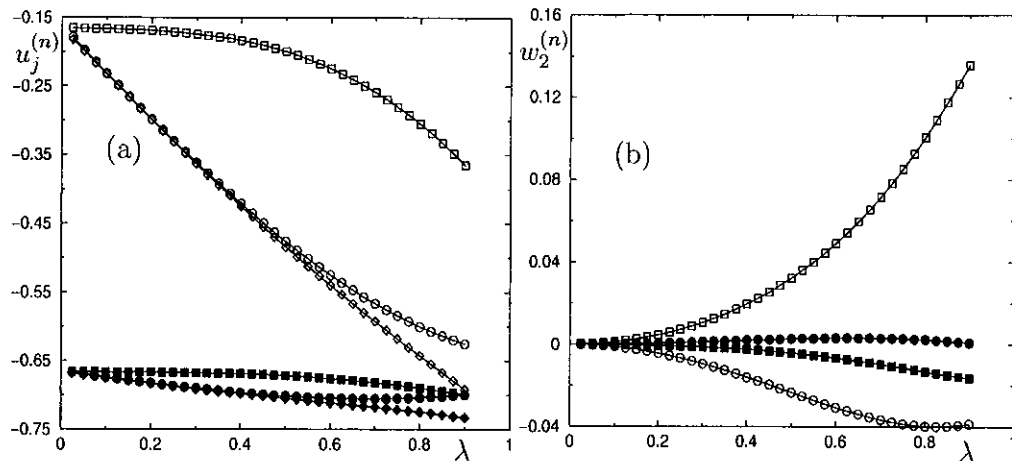Fig. 3. Non-zero mobilities for two inequal spheres with $a_2 = 2a_1 = 2a$: (a) functions $-u_1^{(1)}$ (O) and $-u_1^{(2)}$ (●) in Case 1; $u_1^{(1)}$ (□) and $u_1^{(2)}$ (■) in Case 2; $u_3^{(1)}$ (◇) and $u_3^{(2)}$ (◆) in Case 3; (b) functions $w_2^{(1)}$ (O) and $w_2^{(2)}$ (●) in Case 1; $w_2^{(1)}$ (□) and $w_2^{(2)}$ (■) in Case 2.

Fig. 3. Mobilités non nulles pour deux sphères différentes avec $a_2 = 2a_1 = 2a$: (a) fonctions $-u_1^{(1)}$ (O) et $-u_1^{(2)}$ (●) dans le Cas 1 ; $u_1^{(1)}$ (□) et $u_1^{(2)}$ (■) dans le Cas 2 ; $u_3^{(1)}$ (◇) et $u_3^{(2)}$ (◆) dans le Cas 3 ; (b) fonctions $w_2^{(1)}$ (O) et $w_2^{(2)}$ (●) dans le Cas 1 ; $w_2^{(1)}$ (□) et $w_2^{(2)}$ (■) dans le Cas 2.

big sphere mobility $u_j^{(2)}(\lambda)$ weakly depends upon λ and $1 \leqslant |u_j^{(2)}(\lambda)/u_j^{(2)}(0)| \lesssim 1.1$ in any instance. It is also worth noting that, as the reader may easily check, the relative velocity $U^{(1)} - U^{(2)}$ decreases in magnitude as spheres approach. Finally (see Fig. 3(b)), the only non-zero velocity components $\Omega_2^{(n)}$ exhibit the same trends as the translational velocities components: non-negligible mobilities $w_2^{(n)}(\lambda)$ increase in magnitude with λ, the small sphere rotates faster than the big one in Cases 1 and 2 and the small rotation of the big sphere weakly depends upon both the selected case and the separation parameter λ.

5. Concluding remarks

As illustrated by our numerical results, sphere-sphere interactions always and eventually dramatically speed up each sphere. A 2-sphere cluster will then catch up other single spheres in a separation process. Note that clusters consisting of two insulating ellipsoids centered at O_1 and O_2 should experience a (global) rotation of the vector O_1O_2 (if at least one particle is non-spherical). Particle–particle interactions in such challenging and more involved cases are under current investigation.

References

[1] D. Leenov, A. Kolin, Theory of electromagnetophoresis. I. Magnetohydrodynamic forces experienced by spherical and symmetrically oriented cylindrical particles, J. Chem. Phys. 22 (1954) 683–688.

[2] P. Marty, A. Alemany, Theoretical and experimental aspects of electromagnetic separation, in: H.K. Moffatt, M.R.E. Proctor (Eds.), Metallurgical Applications of Magnetohydrodynamics, Metals Society, pp. 245–259.

[3] H.K. Moffatt, A. Sellier, Migration of an insulating particle under the action of uniform ambient electric and magnetic fields. Part 1. General theory, J. Fluid Mech. 464 (2002) 279–286.

[4] A. Sellier, Migration of an insulating particle under the action of uniform ambient electric and magnetic fields. Part 2. Boundary formulation and ellipsoidal particles, J. Fluid Mech., in press.

[5] A. Sellier, On the low-Reynolds-number motion of a non-conducting particle in uniform electric and magnetic fields, Magnetohydrodynamics, submitted for publication.

[6] C. Pozrikidis, Boundary Integral and Singularity Methods for Linearized Viscous Flow, Cambridge University Press, 1992.

[7] J. Happel, H. Brenner, Low Reynolds Number Hydrodynamics, Martinus Nijhoff, 1973.

[8] M. Bonnet, Boundary Integral Equation Methods for Solids and Fluids, Wiley, 1999.